

Robust Controller for Active Suspension with Hydraulic Dynamics

Yahaya M. Sam and Johari H.S. Osman

Faculty of Electrical Engineering, Universiti Teknologi Malaysia
81310 UTM Skudai, Johor, MALAYSIA.

*yahaya@fke.utm.my

Abstract

The objective of this paper is to present a new control technique for controlling of an active suspension system with hydraulic dynamics for a quarter car model. The purpose of a car suspension system is to improve the riding quality while maintaining good handling characteristics subject to different road profiles. The objective of designing a controller for a car suspension system is to improve the riding quality without compromising on the handling characteristic by directly controlling the suspension forces to suit the road and driving conditions. In order to achieve the desired ride comfort and road handling and to solve the mismatched condition in the system modeling, a proportional-integral sliding mode control technique is presented to deal with the system and uncertainties. Extensive simulations are performed for different road profiles and the results showed that the proposed controller performed well in improving the ride comfort and road handling for the quarter car model using the hydraulically actuated suspension system.

1 Introduction

The development of an active suspension system for a vehicle is of a great interest in both academic and industrial fields. The study of active suspension system has been performed using various suspension models. Generally, a vehicle suspension models are divided into three types: a quarter car, a half car and a full car models. In the quarter car model, the model takes into account the interaction between the quarter car body and the single wheel. Motion of the quarter car model is only in vertical direction. For the half car model, the interactions are between the car body and the wheels and also between both ends of the car body. The first interaction in the half car model caused the vertical motion and the second interaction produced an angular motion. In the full car model, the interactions are between the car body and the four wheels that generate the vertical motion, between the car body and the left and right wheels that generate an angular motion called rolling and between the car body

and the front and rear wheels that produce the pitch motion.

Modeling of the active suspension systems in the early days considered that the input to the active suspension is a linear force. Active suspension with linear force input is presented in [1,2]. Recently, due to the development of new control theories, the force input to the active suspension systems has been replaced by an input to control the actuator. Therefore, the dynamics of the active suspension systems now consists of the dynamics of suspension system plus the dynamic of the actuator systems. Hydraulic actuators are widely used in the active suspension system as presented in [3,4,5,6].

Various control laws such as adaptive control [7], backstepping method [4], optimal state-feedback [1], fuzzy control [6] and sliding mode control [8] have been proposed in the past years to control the active suspension system. The sliding mode control has relatively simpler structure and it guarantees the system stability.

In this paper we will consider a control scheme that can improve further the ride comfort and road handling of the active suspension system. The proposed control scheme differ from the previous sliding mode control techniques in the sense that the sliding surface is based on the proportional-integral sliding mode control instead of the conventional sliding surface.

2 Dynamic model of active suspension

Most of the past active suspension designs were developed based on the quarter-car model as shown in Figure 1, where m_b and m_w are the mass for the car body and car wheel, respectively, k_b and k_w are the stiffness of the car body spring and car tyre, respectively, c_b is the damping constant for the damper, x_b and x_w are the vertical displacement of the car body and the car wheel, respectively, f_a is the control force that generated by the actuating ram in the hydraulic cylinder as presented in [8], and w is an irregular excitation from the road surface. In the model, it is assumed that all the suspension components are linear.

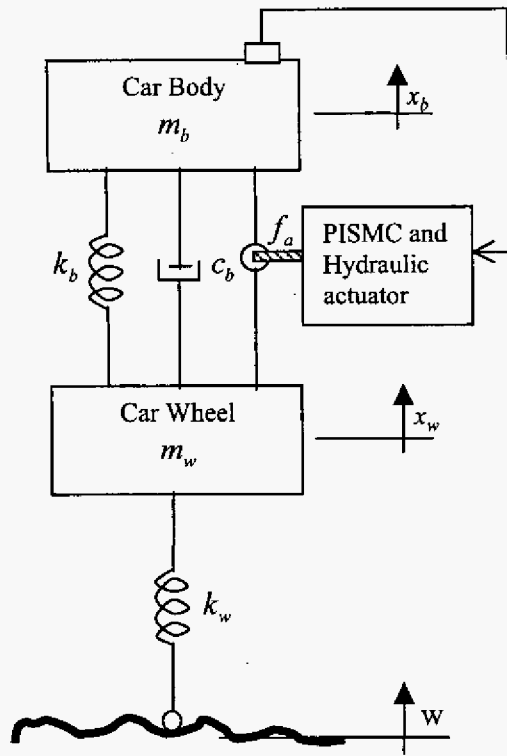


Figure 1: Active Suspension for Quarter Car Model.

From figure 1 the following state-space equation can be easily obtained for the hydraulically actuated active suspension system for quarter car model:

$$\begin{bmatrix} \ddot{x}_b \\ \ddot{x}_w \\ \dot{x}_b \\ \dot{x}_w \\ \dot{f}_a \end{bmatrix} = \begin{bmatrix} -\frac{c_b}{m_b} & \frac{c_b}{m_b} & -\frac{k_b}{m_b} & \frac{k_b}{m_b} & \frac{1}{m_b} \\ \frac{c_b}{m_w} & -\frac{c_b}{m_w} & \frac{k_b}{m_w} & -\frac{(k_b + k_w)}{m_w} & -\frac{1}{m_w} \\ 1 & 0 & 0 & 0 & 0 \\ 0 & 1 & 0 & 0 & 0 \\ -\frac{A_y}{A_e} & \frac{A_y}{A_e} & 0 & 0 & -\frac{1}{A_e} \end{bmatrix} \begin{bmatrix} \dot{x}_b \\ \dot{x}_w \\ x_b \\ x_w \\ f_a \end{bmatrix} + \begin{bmatrix} 0 \\ 0 \\ 0 \\ 0 \\ \frac{1}{A_e} \end{bmatrix} u(t) + \begin{bmatrix} 0 \\ \frac{k_w}{m_w} \\ 0 \\ 0 \\ 0 \end{bmatrix} w(t) \quad (1)$$

A_e and A_y are the hydraulic actuator constants. It can be seen from equation (1) that the system suffer from mismatched condition.

In general, equation (1) can be written in a compact form as

$$\dot{x}(t) = Ax(t) + Bu(t) + f(x, t) \quad (2)$$

where $x(t) \in \mathbb{R}^n$ is the state vector, $u(t) \in \mathbb{R}^m$ is the control input, and the continuous function $f(x, t)$ represents the uncertainties with the mismatched condition. The following assumptions are taken as standard:

Assumption i: There exists a known positive constant such that $\|f(x, t)\| \leq \beta$, where $\|\bullet\|$ denotes the standard Euclidean norm.

Assumption ii: The pair (A, B) is controllable and the input matrix B has full rank.

3 Variable structure control design

In this study, the PI sliding surface define as follows is used:

$$\sigma(t) = Cx(t) - \int_0^t (CA + CBK)x(\tau) d\tau \quad (3)$$

where $C \in \mathbb{R}^{m \times n}$ and $K \in \mathbb{R}^{n \times n}$ are constant matrices. The matrix K satisfies $\lambda_{\max}(A + BK) < 0$ and C is chosen so that CB is nonsingular. The additional integral term provides one more degree of freedom in the design than the conventional sliding surface [9]. This will provide more flexibility in determining the sliding surface and also will reduce the steady-state error.

It is well known that the system is able to enter the sliding mode, $\sigma(t) = 0$ if the reaching condition $\sigma(t)\dot{\sigma}(t) < 0$ is satisfied. During the sliding mode, the equivalent control,

$u_{eq}(t)$ can be obtained by letting $\dot{\sigma}(t) = 0$ [10] i.e.,

$$\dot{\sigma}(t) = C\dot{x}(t) - \{CA + CBK\}x(t) = 0 \quad (4)$$

If the matrix C is chosen such that CB is nonsingular, this yields

$$u_{eq}(t) = Kx(t) - (CB)^{-1}Cf(x, t) \quad (5)$$

Substituting equation (5) into equation (2) gives the equivalent dynamic equation of the system in sliding mode as:

$$\dot{x}(t) = (A + BK)x(t) + \{I_n - B(CB)^{-1}C\}f(x, t) \quad (6)$$

Theorem 1:

If $\|F(x, t)\| \leq \beta_1$ where $\beta_1 = \|I_n - B(CB)^{-1}C\|\beta$

the uncertain system in equation (6) is boundedly stable on the sliding surface $\sigma(t) = 0$.

Proof:

For simplicity, we let

$$\tilde{A} = (A + BK) \quad (7)$$

$$\tilde{F}(x, t) = \{I_n - B(CB)^{-1}C\}f(x, t) \quad (8)$$

and rewrite (6) as

$$\dot{x}(t) = \tilde{A}x(t) + \tilde{F}(x, t) \quad (9)$$

Let the Lyapunov function candidate for the system is chosen as

$$V(t) = x^T(t)Px(t) \quad (10)$$

Taking the derivative of $V(t)$ and substituting equation (6) into it, gives

$$\begin{aligned} \dot{V}(t) &= x^T(t)[\tilde{A}^T P + P\tilde{A}]x(t) + \\ &\quad \tilde{F}^T(x, t)Px(t) \\ &\quad + x^T(t)P\tilde{F}(x, t) \\ &= -x^T(t)Qx(t) + \tilde{F}^T(x, t)Px(t) \\ &\quad + x^T(t)P\tilde{F}(x, t) \end{aligned} \quad (11)$$

where P is the solution of $\tilde{A}^T P + P\tilde{A} = -Q$ for a given positive definite symmetric matrix Q . It can be shown that equation (11) can be reduced to:

$$\dot{V}(t) = -\lambda_{\min}(Q)\|x(t)\|^2 + 2\beta_1\|P\| \|x(t)\| \quad (12)$$

Since $\lambda_{\min}(Q) > 0$, consequently $\dot{V}(t) < 0$ for all t and $x \in B^c(\eta)$, where $B^c(\eta)$ is the complement of the closed ball $B(\eta)$, centered at $x = 0$ with radius $\eta = \frac{2\beta_1\|P\|}{\lambda_{\min}(Q)}$.

Hence, the system (2) is uniformly ultimately bounded. \square

Remark2: For the system with uncertainties satisfying the matching condition, i.e., $\text{rank}[B \mid f(x, t)] = \text{rank}[B]$, then

equation (6) can be reduced to $\dot{x}(t) = (A + BK)x(t)$ [11]. Thus asymptotic stability of the system during sliding mode is assured.

The control scheme that drives the state trajectories of the system in equation (2) onto the sliding surface $\sigma(t) = 0$ and the system remains in it thereafter is now be designed. For the uncertain system in equation (2) satisfying assumptions (i) and (ii), the following control law is proposed:

$$u(t) = Kx(t) - (CB)^{-1}Cf(t) - (CB)^{-1}\rho \frac{\sigma(t)}{|\sigma(t)| + \delta} \quad (13)$$

where K is a vector of closed loop gains, ρ and δ are the design constants.

The state trajectories that are driven by the above controller will slide on the designed sliding surface if the reaching condition $\sigma(t)\dot{\sigma}(t) < 0$ is satisfied. To evaluate the reaching condition, we express,

$$\sigma(t)\dot{\sigma}(t) = \sigma(t)[CBu(t) + Cf(x, t) - CBKx(t)] \quad (14)$$

Substituting equation (13) into equation (14), gives

$$\sigma(t)\dot{\sigma}(t) = \sigma(t) \left[-\rho \frac{\sigma(t)}{|\sigma(t)| + \delta} \right] \quad (15)$$

Equation (15) shows that the hitting condition of the sliding surface (3) is satisfied if $\rho > 0$.

4 Simulations and discussion

The mathematical model of the system as defined in equation (2) and the proposed PI sliding mode controller (PISMC) in equation (13) were simulated on computer. Numerical values for the model parameters are taken from [8], and are as follows:

$$\begin{aligned} M_s &= 290 \text{ kg}, M_{us} = 59 \text{ kg}, K_a = 16812 \text{ N/m} \\ K_t &= 190000 \text{ N/m}, C_a = 1000 \text{ N/(m/sec)} \end{aligned}$$

Two sets of road profiles were used in the simulation: Road profile RP2:

$$w(t) = \begin{cases} a(1 - \cos 8\pi t), & 1.25 \text{ sec} \leq t \leq 1.5 \text{ sec} \\ 0, & \text{otherwise} \end{cases}$$

and Road profile RP4:

$$w(t) = \begin{cases} a(1 - \cos 8\pi t), & 1.25 \text{ sec} \leq t \leq 1.5 \text{ sec}, \\ & 3.00 \text{ sec} \leq t \leq 3.25 \text{ sec}, \\ & 5.00 \text{ sec} \leq t \leq 5.25 \text{ sec}, \\ & 7.00 \text{ sec} \leq t \leq 7.25 \text{ sec}, \\ & 9.00 \text{ sec} \leq t \leq 9.25 \text{ sec}, \\ 0, & \text{otherwise} \end{cases}$$

a denotes the bump amplitude where $a = 11 \text{ cm}$ is used. The road profiles RP2 and RP4 are shown in figures 2(a) and 3(a) respectively. These types of road profiles have been used by [4,12] in their studies. Furthermore, the maximum travel distance of suspension travel of $\pm 8 \text{ cm}$ as suggested by [4] has been considered. For the PISMC, we utilize the pole placement method to determine the value of K such that $\lambda(A + BK) = \{-50, -100, -110, -120, -500\}$. This yields $K = [-1.65e8 \ -1.88e7 \ -3.34e9 \ 1.08e9 \ -970.35]$. In the

simulation the following values were selected for the respective controller parameters: $C = [3 \ 2 \ 5 \ 10 \ 30]$, $\rho = 10$, $\delta = 1e-2$, $A_y = 15$ and $A_e = 1.13$.

In order to fulfill the objective of designing an active suspension system i.e. to increase the ride comfort and road handling, there are two parameters to be observed in the simulations. The two parameters are the car body acceleration and wheel deflection. Figures 2(b) and 3(b) show the suspension travel under the active suspension system and a passive suspension system for both road profiles. The passive suspension system is included as comparison purposes. The result shows that the suspension travel is within the travel limit i.e. $\pm 8\text{cm}$. Moreover the wheel deflections as shown in figures 2(c) and 3(c) are also smaller using the proposed controller. Figures 2(d) and 3(d) illustrate clearly how the PISMC can effectively absorb the vehicle vibration in comparison to the passive system. The body acceleration in PISMC design system is reduced significantly, which guarantees better ride comfort. Figures 2(e) and 3(e) shows that the sliding conditions are fulfilled, that is the states trajectories slide on the sliding surface i.e. at $\sigma = 0$ and remains thereafter. The control input signals to the system are as shown in figures 2(f) and 3(f). Therefore, it is concluded that the active suspension system with the PISMC improves the ride comfort while retaining the road handling characteristics, as compared to the passive suspension system.

5 Conclusion

This paper presents a methodology to design a controller for an active suspension system integrated with hydraulic dynamics that is based on variable structure control theory, which is capable of satisfying all the pre-assigned design requirements within the actuators limitation. A detailed study of the proportional integral sliding mode control algorithm is presented. The performance characteristics of the active suspension systems is evaluated and then compared with the passive suspension system through computer simulation.

The result shows that the use of the proposed proportional integral sliding mode control technique proved to be effective in controlling vehicle vibrations and achieve better performance than the passive suspension system.

Acknowledgement

The authors wish to express sincere gratitude to Professor T. Yoshimura from Tokushima University for his contributions in this research.

References

- [1] Esmailzadeh E. and Taghirad H.D. *Active Vehicle Suspensions with Optimal State-Feedback Control*. Journal of Mechanical Science, Vol. 200, No. 4, pp. 1- 18, 1996.
- [2] Huang, S. J. and Chao, H. C. *Fuzzy Logic Controller for Active Suspension System*. Proc. Instn. Mech. Engrs. Vol. 214, Part D, pp. 1-12, 2000.
- [3] Alleyne A. and Hedrick J.K. *Nonlinear Adaptive Control of Active Suspensions*. IEEE Trans. Control System Technology. Vol. 3, pp. 94-101, 1995.
- [4] Lin J.S. and Kanellakopoulos I. *Nonlinear Design of Active Suspension*. IEEE Control System Magazine. Vol.17, pp. 45-59, 1997.
- [5] Fialho, I. and Balas, G.J. *Road Adaptive Active Suspension Design using Linear Parameter-Varying Gain-Scheduling*. IEEE Transaction on Control Systems Technology, Vol. 10, No. 1, pp. 43-54, 2002.
- [6] Yoshimura T., Nakaminami K., Kurimoto M. and Hino J. *Active suspension of passengers cars using linear and fuzzy-logic controls*. Control Engineering Practice, Vol. 7, pp. 41-47, 1999.
- [7] Appleyard M. and Wellstead P.E. *Active suspension : some background*. Proc. Control Theory Applications. Vol. 142, pp. 123-128, 1995.
- [8] Yoshimura T., Kume A., Kurimoto M. and Hino J. *Construction of an active Suspension system of a quarter car model using the concept of sliding mode control*. Journal of Sound and Vibration, Vol. 239, pp. 187-199, 2001.
- [9] Cao W.J. and Xu J.X. *Nonlinear Integral-type Sliding Surface for Both Matched and Unmatched Uncertain Systems*, Proceedings of the American Control Conference, 25-27 June 2001, pp. 4369-4374.
- [10] Itkis U. *Control System of Variable Structure* Wiley, New York, 1976.
- [11] Edward C. and Spurgeon S. *Sliding Mode control: Theory and Applications*, Taylor and Francis, London, 1988.
- [12] D'Amato F.J. and Viasallo D.E. *Fuzzy Control for Active Suspensions*. Mechatronics. Vol. 10, pp. 897-920, 2000.

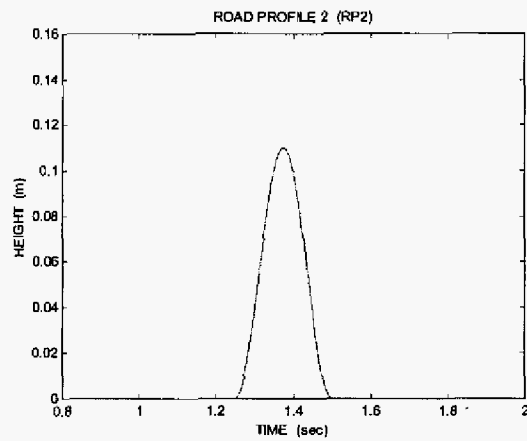


Figure 2(a): Road profile RP2

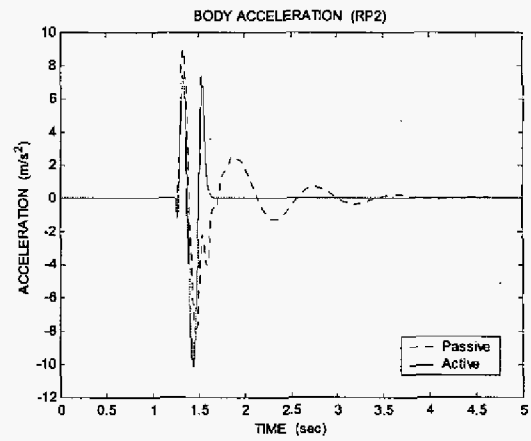


Figure 2(d): Body acceleration for RP2

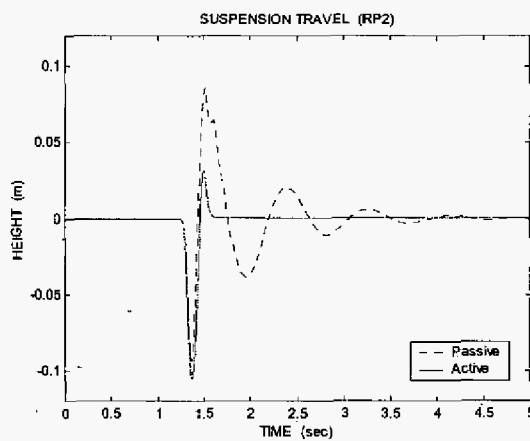


Figure 2(b): Suspension travel for RP2

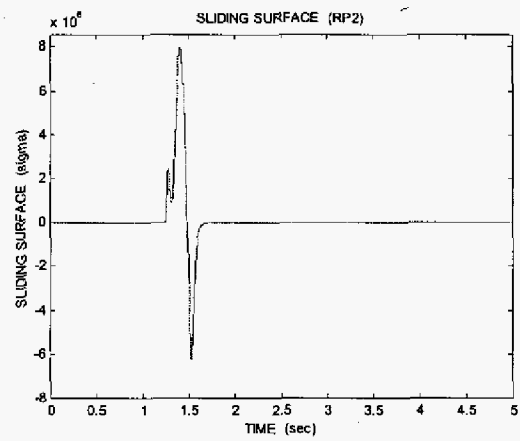


Figure 2(e): Sliding surface for RP2

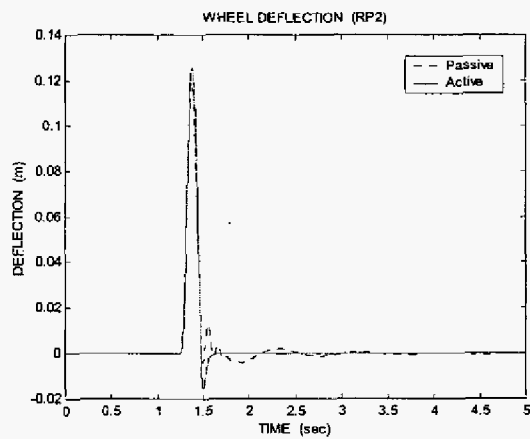


Figure 2(c): Wheel deflection for RP2

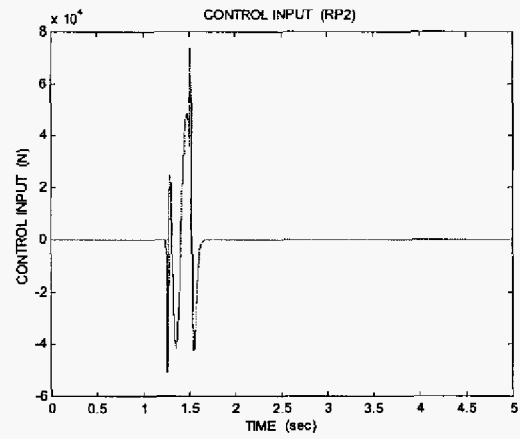


Figure 2(f): Control input for RP2

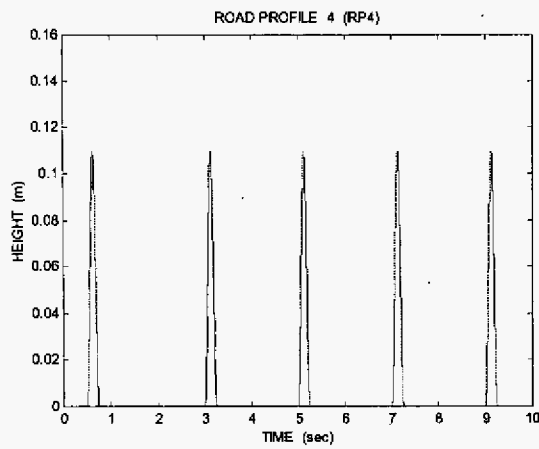


Figure 3(a): Road profile RP4

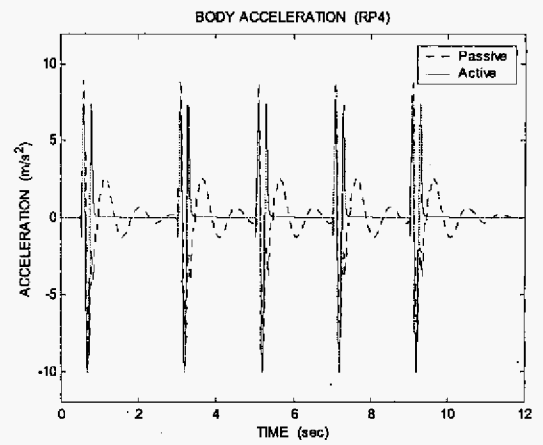


Figure 3(d): Body acceleration for RP4

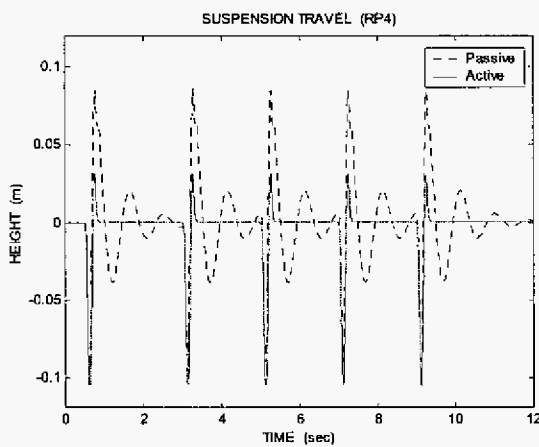


Figure 3(b): Suspension travel for RP4

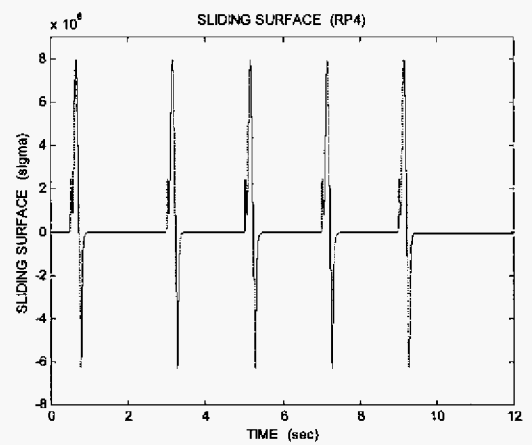


Figure 3(e): Sliding surface for RP4

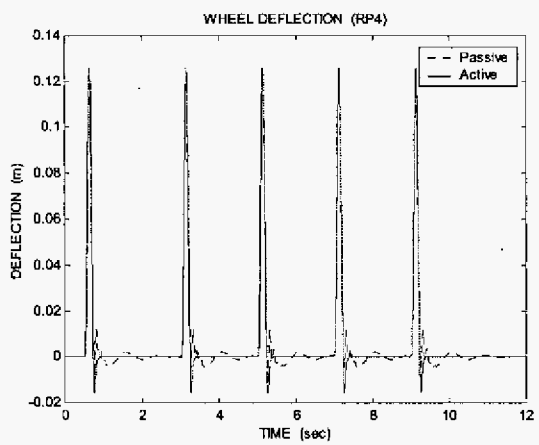


Figure 3(c): Wheel deflection for RP4

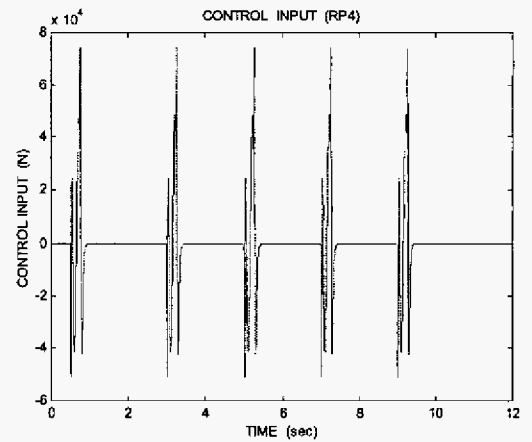


Figure 3(f): Control input for RP4